The effect of plasma nitriding on the synergism between wear and corrosion of SAF 2205 duplex stainless steel

Yamid Núñez, Marcio Mafra, Rigoberto E. Morales, Paulo César Borges and Giuseppe Pintaude
Department of Mechanics, Universidade Tecnológica Federal do Paraná, Curitiba, Brazil

Abstract

Purpose – This study aims to assess the performance of SAF 2205 duplex stainless steel against pure wear, tribo-corrosion, corrosion and the synergism between wear and corrosion. The effect of plasma nitriding conducted at low temperature (380°C) on SAF 2205 steel was analyzed.

Design/methodology/approach – Three systems were used for assessing the synergism between wear and corrosion: tribo-corrosion – wear tests conducted using the micro-scale abrasion test, performed under a slurry of alumina particles containing 3.5% NaCl; pure wear – tests conducted using the previous system but isolated in a glovebox with a 99% N2 atmosphere; and cyclic polarization under 3.5% NaCl solution. A hard nitrided layer of 3 μm thickness was characterized using X-ray diffraction, presenting expanded austenite.

Findings – The wear mode after micro-scale abrasion tests changed in the absence of an oxygen atmosphere. During pure wear, a mixed mode was identified (rolling + grooving), with the grooving mode more intense for the untreated steel. For tribo-corrosion tests, only rolling wear was identified. For all cases, the nitrided samples presented less wear. The corrosion results indicated a higher repassivation potential for the nitrided condition.

Practical implications – The synergism was more positive for the nitrided sample than for the untreated one, which can be considered for surface treatments of duplex stainless steels in practical applications.

Originality/value – A detailed description of wear mechanisms showed a significant change in the presence of oxygen atmosphere, a new approach for isolating pure wear.

Keywords Duplex stainless steel, Plasma nitriding, Micro-abrasion, Corrosion, Tribo-corrosion, Synergistic effect

Paper type Research paper

1. Introduction

Duplex stainless steel has been successfully used in the oil and gas industry (Craidy *et al.*, 2015). Among its applications are joints, valves and pipes subject to aggressive medium. Such components can suffer degradation from the interaction with the saline environment and at the same time with the sand present in the seawater.

The improvement of abrasion resistance can be achieved by using surface treatments, such that the hardness of duplex stainless steel is limited to restrictions imposed by the possibility of hydrogen embrittlement (Lai *et al.*, 2013). In this way, low-temperature plasma nitriding is an alternative for keeping the corrosion resistance and improving the surface hardness (Cardoso *et al.*, 2016) and probably mitigating the hydrogen embrittlement (Asgari *et al.*, 2013).

The abrasion behavior of duplex stainless steels has been studied separately from their corrosion resistances (Marques *et al.*, 2011; Pereira Neto *et al.*, 2016; Pintaude *et al.*, 2019).

Marques *et al.* (2011) studied the micro-abrasion and corrosion behaviors of super duplex UNS S32750 steel. They observed that the precipitation of a hard phase after heat treatment increased the wear resistance by 50 per cent. The harder sample, containing sigma phase, presented less wear, associated with shallower grooves and fewer indentations on the hard phase. However, this condition resulted in a significant drop in the critical pitting temperature and fracture toughness. On the other hand, in the presence of α' phase (nanometric Cr-rich precipitates) the increase in wear was not accompanied either with less corrosion or even toughness reductions.

The effect of plasma nitriding on the wear and corrosion behaviors was described by Pereira Neto *et al.* (2016) separately. In their study, the crater wear was caused by direct contact between the ball and the worn surface, without a slurry. Within the range of nitriding temperatures (350-570°C), they

The current issue and full text archive of this journal is available on Emerald Insight at: **https://www.emerald.com/insight/0036-8792.htm**

Industrial Lubrication and Tribology
72/9 (2020) 1117–1122

[DOI 10.1108/ILT-08-2019-0302]

The authors would like to thank funding given by National Council for Scientific and Technological Development (CNPq) (Process 443896/2014-3) and Fundação Araucária (Process FA CP08/2017) for their financial support. The authors also thank the Multi-User Center for Materials Characterization (CMCM, Curitiba, Brazil) scanning electron microscopy analysis and Sandvik do Brasil S/A (São Paulo, Brazil) for supplying duplex stainless steel bars. One of authors, G. Pintaude, thanks to CNPq by the financial support through Process 308416/2017-1.

Received 2 August 2019
Revised 15 November 2019
Accepted 9 January 2020

found that 400°C can be allied with wear and corrosion resistances.

Pintaude *et al.* (2019) studied the effect of low-temperature plasma nitriding (380°C) on the scratch resistance and corrosion of two grades of duplex stainless steel (SAF 2205 and SAF 2507). The higher support given by the hardness of SAF 2507 steel was determinant for achieving a larger critical load in the scratch test for a thin layer composed by expanded austenite, formed due to plasma nitriding. In terms of corrosion, the pitting potential was practically unchanged after nitriding.

There are many adaptations to conduct micro-scale abrasive wear tests and corrosion at the same time. The works of Stack *et al.* (2010) and Sun *et al.* (2009) revealed that the test parameters of micro abrasion-corrosion adapted test rig affect the wear mechanism of biomedical alloys, being possible to evidence the transitions between them. They highlighted the crucial influence of the formation and breakdown of a passivation film on the degradation mechanism and synergy effect.

A similar approach to that developed in the current study was introduced by Bello *et al.* (2007). These authors considered three systems:

1 pure abrasion, using a slurry diluted in distilled water;
2 abrasion-corrosion, using a slurry diluted in a corrosive 3.5 per cent NaCl solution; and
3 the corrosion component enhanced by abrasion, where the ball-cratering rig with no SiC abrasive slurry but only using the 3.5 per cent NaCl solution.

They studied three stainless steels: UNS S30403, S31603 and S32760 grades. The S32760 grade delivered the best repassivation performance with negative synergistic characteristics.

More recently, Santos *et al.* (2015) developed a new test rig that consists of a fixed-ball micro-abrasion tester, which had the unique capability of monitoring the forces acting on the contact of abrasion-corrosion processes. They studied an austenitic (AISI 304) and ferritic (AISI 430) stainless steels, obtaining negative synergy on tribo-corrosion conditions for both steels. Their approach also involved studying the same three systems as Bello *et al.* (2007), but with SiO_2 particles and 1 N H_2SO_4 corrosive solution.

To our knowledge, the approach used by Bello *et al.* (2007) and Santos *et al.* (2015) was not still explored for surface-treated duplex stainless steels. Considering these previous investigations, the current study aims to present the effect of low-temperature plasma nitriding on the synergism between abrasion and corrosion, using a different approach from Bello *et al.* (2007) and Santos *et al.* (2015) to produce pure abrasion.

2. Experimental procedures

Samples of super duplex stainless steel SAF 2205 (~3 per cent Mo, 22 per cent Cr, and 5 per cent Ni) were extracted from a bar of 85.5-mm diameter. The cutting process was used to obtain coupons with dimensions of 5 x 20 x 60 mm. After cutting, the specimens were ground and subsequently sanded for a finishing equivalent to a sandpaper #600 grit. Its Vickers hardness is 368 ± 36 $HV_{0.05}$.

2.1 Plasma nitriding

After sanding, the samples were washed and cleaned properly for the plasma nitriding treatment, conducted in a pulsed DC reactor. The treatment consists in two steps:

1 an initial sputtering for 20 min under a gas mixture of (25%Ar-75%H_2) at 300°C, for removing the passive layer; and
2 nitriding for 10 h under a gas mixture of (25%N_2-75%H_2), at 380°C.

The temperature and time of nitriding treatment were based on a previous investigation (Pintaude *et al.*, 2019). During all steps, the pressure and voltage were kept constant at 3 Torr (400 Pa) and 600 V, respectively. The parameters plasma-on and plasma-off periods were controlled for assuring a maximum variation for the temperature of ±2°C.

2.2 Characterization of nitrided specimens

The microstructure of the nitrided layer was revealed for assessing its thickness, etching polished cross-sections with oxalic acid 10 per cent Vol. in an electrolytic device. The phases of the nitrided layer were analyzed using X-ray diffraction (XRD). The top hardness of layers was determined through the Vickers scale, using 490 mN. The average values corresponded to a series of 10 measurements.

2.3 Pure wear (W_0) and tribo-corrosion (T) evaluation

The evaluation of wear without corrosion (W_0) and tribo-corrosion (T) was performed through a micro-scale abrasion test rig, using a free-ball configuration. As a counter-body, a ball of zirconia of 24.5-mm diameter (52.14 g of mass) was employed. The slurry was composed of a water suspension containing 20 per cent m/v of alumina particles, with d_{50} = 6.7 ± 0.3 μm (Rovani *et al.*, 2019), dissolved in depleted distilled water. For the tribo-corrosive tests, 3.5 per cent of NaCl was added to the slurry. For controlling the corrosion, the test rig was placed into a glovebox (Figure 1). The glovebox volume was filled with nitrogen gas (99.999 per cent minimum) using a flow rate of 10 L/min. After that, the minimum content of nitrogen was controlled using a flow rate of 1 L/min. Using an optical spectrometer, the peak of 844.1 nm, corresponded to the oxygen gas, was monitored to guarantee a maximum of 1 per cent of oxygen inside the chamber. On the opposite, the tribo-corrosive tests were carried out in an open-to-air environment.

Figure 1 Schematic drawing of glovebox, showing the system used for reproducing wear without corrosion

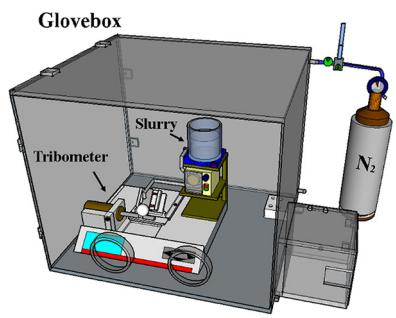

Testing variables used for micro-scale abrasion tests were: a dynamic load of 0.1 N, an axis rotation speed of 300 rpm, a testing time of 18 min, and a drop rate of ~2 ml/min. These parameters were used elsewhere (Rovani *et al.*, 2019) and they assured that all tests were performed within the steady-state regime of wear. For each testing condition, four measurements were done.

2.4 Corrosion evaluation C_0

Potential-dynamic tests were performed for evaluating the corrosion behavior of the SAF 2205 steel before and after the plasma nitriding. The corrosion rate was calculated considering the Tafel region. Tests were carried out using scanning of potentials in the anodic direction, using a scan rate of 1 mV/s, from 0.3 V below the rest potential up to 1.5 V (reversion point), and finally returning to the initial value of potential. To obtain average values of corrosion parameters, five experiments were carried out at least.

2.5 Synergism evaluation (S)

Figure 2 is a flow chart detailing all tests performed in this work. The values of wear rate without corrosion (W_0) and tribo-corrosion (T) and the value of corrosion rate (C_0) obtained on each test procedure were used for synergism calculation. The synergism between wear and corrosion was calculated following the recommendations of ASTM G119-09 Standard.

$$S = T - W_0 - C_0 \quad (1)$$

3. Results and discussion

Figure 3 shows the cross-section of nitrided SAF 2205 steel. A continuous and uniform layer can be observed, with an average value of the thickness of 3.0 ± 0.2 μm. This layer is constituted by a metastable phase so-called S-phase or expanded austenite, which had been confirmed by following XRD results.

Figure 2 Flow chart detailing the tests performed

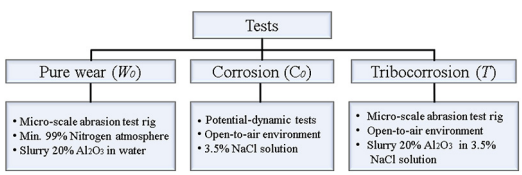

Figure 3 Cross-section of nitrided SAF 2205 steel (380°C for 10 h)

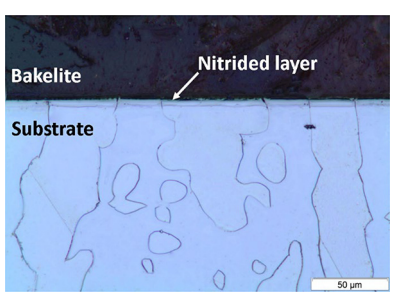

After plasma nitriding, the Vickers hardness of the surface is 1102 ± 178 $HV_{0.05}$. Thus, the surface treatment was able to increase three times the initial hardness. However, this value can be underestimated yet, considering the indentation depth achieved during the test – approximately 1.32 μm – which corresponds to 44 per cent of layer thickness. This percentage is high enough for the substrate properties had influenced the hardness.

Figure 4 shows the spectrum of XRD for the untreated and nitrided conditions. As expected, the diffractogram relative to the untreated specimen [Figure 4(a)] presents only peaks associated with the austenite (γ-Fe) and ferrite (α-Fe). On the other hand, in the nitrided specimens, one can observe the disappearing of peaks relative to the ferrite and a shift of peaks 1 and 3 [Figure 4(b)], related to the austenite, for smaller angles (peaks I and II). The peaks identified as I and II have been related to the expanded austenite, sometimes called as S-phase, as described by Alphonsa *et al.* (2015) and Cardoso *et al.* (2016). This shift is associated with the increase in the lattice parameter of austenite, caused by the nitrogen supersaturation (Pinedo *et al.*, 2013).

Table I presents the wear rates for systems corresponding to the abrasive wear without corrosion (W_0) and tribo-corrosion (T). For both material conditions, the wear produced by tribo-corrosion is higher than that observed for the pure wear, indicating the effect of corrosive component for both superficial conditions. The presence of an expanded austenite layer caused a reduction of 50.6 per cent in the pure

Figure 4 (a) XRD spectrum of untreated SAF 2205 steel, presenting peaks of austenite (2, 3) and (b) XRD spectrum of nitrided SAF 2205 steel, showing peaks of expanded austenite (I, II)

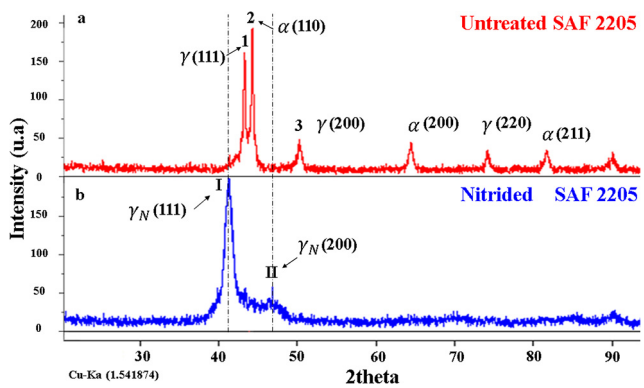

Table I Wear rates (mm/year) of SAF 2205 steel for pure wear (W_0) and tribo-corrosion (T) testing conditions, before and after plasma nitriding

Condition	Wear rate (mm/year)
Untreated SAF 2205 steel	
T	11.5 ± 0.3
W_0	8.3 ± 0.3
Nitrided SAF 2205 steel	
T	9.5 ± 0.4
W_0	4.2 ± 0.6

wear and 17.4 per cent in the tribo-corrosion wear rate. Although the benefit of plasma nitriding is observed for both tribo-systems, the expanded austenite reduced much more the wear without corrosion.

Figure 5 presents the worn surfaces revealed in SEM before and after plasma nitriding. The images correspond to the center of craters. Some grooves and indentations marks are indicated by dotted yellow and green lines, respectively. In Figure 5(a) the combined presence of grooves and indentations can be observed, which correspond to the mixed mode of wear, being the grooving more intense for the untreated steel under pure wear. Surprisingly, another situation was found when the SAF 2205 steel was subject to tribo-corrosive system [Figure 5{b)]. The rolling mode of wear became predominant, indicating that the presence of a passive layer could be decisive for the mode of wear.

Figure 5(c) shows the worn surface of the nitrided layer under pure wear condition. In comparison with the untreated steel, the presence of a hard layer acted for reducing the occurrence of grooves. This observation meets the wear rates presented in Table II, where a significant reduction was noted due to the nitrided layer; however, a mixed mode of wear was also presented. In the same sense of abovementioned for the untreated SAF 2205 steel, the change of system from pure abrasion to tribo-corrosion changed the mode of wear, i.e. in Figure 5(d) one can observe the predominance of rolling mode of wear.

Changes in the wear mode during the micro-scale abrasion test can be associated with different width of the wear caused by the abrasive particles (Da Silva and De Mello, 2009). This relation was described in detail by Rovani *et al.* (2019). These authors identified a significant reduction in the λq parameter (~the width of wear track) when the mixed mode changed to grooving mode. This roughness parameter was more sensitive to indicate this kind of change than the Sq (root mean square height).

In Figure 6 one can see the curves obtained in cyclic polarization, and in Table II the average values of corrosion potential (E_{corr}), corrosion current (i_{corr}), corrosion rate (C_0), pitting potential (E_p), and the repassivation potential (E_r) can be found.

Analyzing these results, it is possible to check that the corrosion potential of the nitrided condition is worse than the untreated one. However, the values of corrosion current and corrosion rate are equivalent, considering the standard deviations. For the localized corrosion, the pitting nucleation and the repassivation

Table II Corrosion parameters determined after cyclic polarization for untreated and nitrided SAF 2205 steel

Corrosion parameters	Untreated SAF 2205 steel	Nitrided SAF 2205 steel
i_{corr} (μA/cm^2)	0.75 ± 0.52	3.3 ± 2.6
E_{corr} (mV vs SCE)	−150 ± 90	−347 ± 10
E_p (mV)	1010 ± 70	1240 ± 20
E_r (mV)	897 ± 130	1170 ± 30
C_0 (mm/year)	(0.8 ± 0.4) ×10^{-2}	(3.6 ± 3.0) ×10^{-2}

Figure 5 Worn surfaces revealed in SEM

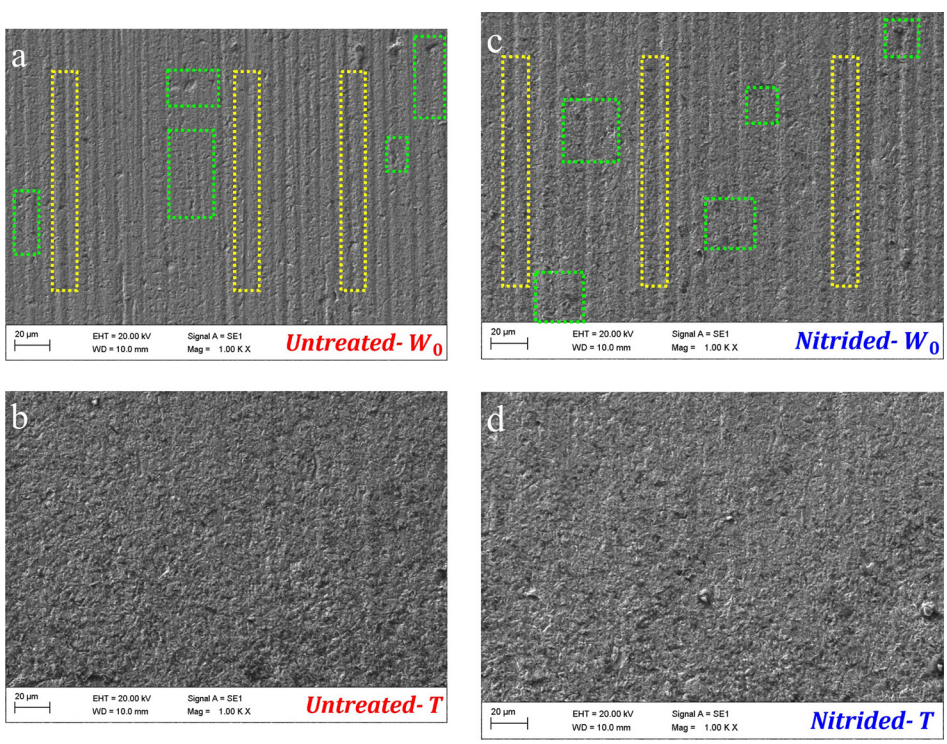

Notes: (a), (b) Untreated SAF 2205 steel, pure wear and tribo-corrosion, respectively; (c), (d) nitrided 2205 steel, pure wear and tribo-corrosion, respectively

Figure 6 Cyclic polarization curves of SAF 2205 steel

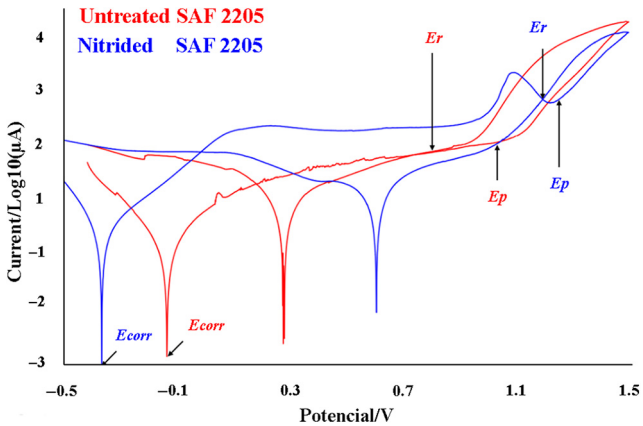

Notes: Untreated (red); nitrided (blue)

potentials are larger with the plasma nitriding, which represents a better-localized corrosion resistance and a small resistance to repassivation, compared with the untreated condition.

Besides the bigger size of the area of hysteresis loop means more passive film breakdown and consequently, more difficulty for restoring the damaged passive film. As shown on the curves in Figure 6, this area is higher for the untreated condition which indicates the higher resistance to repassivation. This result agrees with the literature (Jargelius-Pettersson, 1999), which relates that the presence of nitrogen favors the formation of NH^{+4}, with consequent reduction of pH within the pitting, as well as an easier repassivation verified by the increase of repassivation potential in nitrogen-enriched samples.

Table III shows the values calculated from equation (1) representing the synergistic effect produced by micro-scale abrasion test with, pure micro-scale abrasion test with corrosion and pure corrosion for SAF2205 steel samples before and after plasma nitriding.

Figure 7 presents a summary for better visualization of pure wear (W_0), tribo-corrosion (T), corrosion (C_0) and synergism (S) for the studied surfaces. These data allow verifying that the sum of pure wear and corrosion components is lesser than the tribo-corrosion component. Therefore, the synergism is positive, indicating that the simultaneous action of abrasion and corrosion intensified the wear. The main beneficial effect of plasma nitriding was on pure wear, related to the surface hardness increase.

As the synergism between wear and corrosion is a real problem in duplex stainless steels applied on offshore oil and gas facilities (Aribo *et al.*, 2013), the low-temperature plasma nitriding process can be a good approach for improving the

Table III Synergism (S) (mm/year) values of SAF 2205 steel before and after plasma nitriding

Condition	Synergism S (mm/year)
Untreated SAF 2205 steel	3.2 ± 0.6
Nitrided SAF 2205 steel	5.3 ± 1.0

Figure 7 Diagram presenting the components of tribo-corrosion (T), pure wear (W_0), pure corrosion (C_0) and synergism (S) for the untreated and nitrided SAF 2205 steel

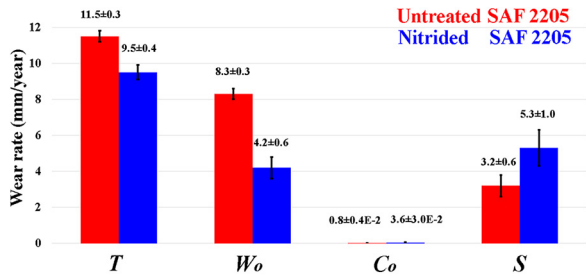

wear and corrosion resistances. According to the results obtained in the present work, the nitrided steel presented a lower wear rate compared to the untreated material in pure wear and tribo-corrosion conditions.

4. Conclusions

Micro-scale abrasion tests were performed with and without control of the corrosion component, allowing to describe the synergism between wear and corrosion for the SAF 2205 steel. From the experimental results, the following conclusions can be put forward:

- The plasma nitriding at low-temperature promotes the formation of a continuous layer of expanded austenite with 3-μm thick; the plasma nitriding promoted an increase in the hardness of SAF 2205 steel from 368 $HV_{0.05}$ to 1102 $HV_{0.05}$.
- The mode of wear changes from the pure abrasion to tribo-corrosion condition, while in the former a mixed mode is observed, the rolling mode was predominant during the tribo-corrosive tests.
- The presence of an expanded austenite layer caused a reduction of 50.6 per cent in the pure wear and 17.4 per cent in the tribo-corrosion wear rate.
- Plasma nitriding improves the resistance to the localized corrosion; the synergism value indicates a positive action for both nitride and untreated samples, indicating that the corrosion is determinant for the tribo-corrosive wear. The synergism was more positive for the nitrided sample than the untreated one.

References

Alphonsa, J., Raja, V.S. and Mukherjee, S. (2015), "Study of plasma nitriding and nitrocarburizing for higher corrosion resistance and hardness of 2205 duplex stainless steel", *Corrosion Science*, Vol. 100, pp. 121-132.

Aribo, S., Barker, R., Hu, X. and Neville, A. (2013), "Erosion–corrosion behaviour of lean duplex stainless steels in 3.5% NaCl solution", *Wear*, Vol. 302 Nos 1/2, pp. 1602-1608.

Asgari, M., Johnsen, R. and Barnoush, A. (2013), "Nanomechanical characterization of the hydrogen effect on pulsed plasma nitrided super duplex stainless steel",

International Journal of Hydrogen Energy, Vol. 38 No. 35, pp. 15520-15531.

Bello, J.O., Wood, R.J.K. and Wharton, J.A. (2007), "Synergistic effects of micro-abrasion–corrosion of UNS S30403, S31603 and S32760 stainless steels", *Wear*, Vol. 263 Nos 1/6, pp. 149-159.

Cardoso, R.P., Mafra, M. and Brunatto, S.F. (2016), "Low-temperature thermochemical treatments of stainless steels – an introduction, chapter 4", *An Introduction, Plasma Science and Technology – Progress in Physical States and Chemical Reactions*, IntechOpen, pp. 107-130.

Craidy, P., Briottet, L. and Santos, D. (2015), "Hydrogen–microstructure–mechanical properties interactions in super duplex stainless steel components", *International Journal of Hydrogen Energy*, Vol. 40 No. 47, pp. 17084-17090.

Da Silva, W.M. and De Mello, J.D.B. (2009), "Using parallel scratches to simulate abrasive wear", *Wear*, Vol. 267 No. 11, pp. 1987-1997.

Jargelius-Pettersson, R.F.A. (1999), "Electrochemical investigation of the influence of nitrogen alloying on pitting corrosion of austenitic stainless steels", *Corrosion Science*, Vol. 41 No. 8, pp. 1639-1664.

Lai, C.L., Tsay, L.W. and Chen, C. (2013), "Effect of microstructure on hydrogen embrittlement of various stainless steels", *Materials Science and Engineering: A*, Vol. 584, pp. 14-20.

Marques, F., Da Silva, W.M., Pardal, J.M., Tavares, S.S.M. and Scandian, C. (2011), "Influence of heat treatments on the micro-abrasion wear resistance of a superduplex stainless steel", *Wear*, Vol. 271 Nos 9/10, pp. 1288-1294.

Pereira Neto, J.O., Silva, R.O.D., Silva, E.H.D., Moreto, J.A., Bandeira, R.M., Manfrinato, M.D. and Rossino, L.S. (2016), "Wear and corrosion study of plasma nitriding F53 super duplex stainless steel", *Materials Research*, Vol. 19 No. 6, pp. 1241-1252.

Pinedo, C.E., Varela, L.B. and Tschiptschin, A.P. (2013), "Low-temperature plasma nitriding of AISI F51 duplex stainless steel", *Surface and Coatings Technology*, Vol. 232, pp. 839-843.

Pintaude, G., Rovani, A.C., das Neves, J.C.K., Lagoeiro, L.E., Li, X. and Dong, H.S. (2019), "Wear and corrosion resistances of active screen plasma-nitrided duplex stainless steels", *Journal of Materials Engineering and Performance*, Vol. 28 No. 6, pp. 3673-3682.

Rovani, A., Rosso, T. and Pintaude, G. (2019), "On the use of microscale abrasion test for determining the particle abrasivity", *Journal of Testing and Evaluation*, Vol. 49, In press, available at: https://doi.org/10.1520/JTE20180576

Santos, M., Labiapari, W., Narvaez Ardila, M., Da Silva Junior, W. and de Mello, J.D.B. (2015), "Abrasion-corrosion: new insights from force measurements", *Wear*, Vols 332/333, pp. 1206-1214.

Stack, M.M., Rodling, J., Mathew, M.T., Jawan, H., Huang, W., Park, G. and Hodge, C. (2010), "Micro-abrasion–corrosion of a Co–Cr/UHMWPE couple in ringer's solution: an approach to construction of mechanism and synergism maps for application to bio-implants", *Wear*, Vol. 269 Nos 5/6, pp. 376-382.

Sun, D., Wharton, J.A. and Wood, R.J.K. (2009), "Micro-abrasion mechanisms of cast CoCrMo in simulated body fluids", *Wear*, Vol. 267 No. 11, pp. 1845-1855.

Further reading

ASTM G119-89 (2015), Standard Practice for Calculation of Corrosion Rates and Related Information from Electrochemical Measurements, ASTM International.

Corresponding author

Giuseppe Pintaude can be contacted at: giuseppepintaude@gmail.com